

Photodissociation dynamics of the allyl radical

Hans-Jürgen Deyerl, Ingo Fischer, and Peter Chen

Citation: *The Journal of Chemical Physics* **110**, 1450 (1999); doi: 10.1063/1.478020

View online: <http://dx.doi.org/10.1063/1.478020>

View Table of Contents: <http://scitation.aip.org/content/aip/journal/jcp/110/3?ver=pdfcov>

Published by the [AIP Publishing](#)

Articles you may be interested in

[D atom loss in the photodissociation of the DNCN radical: Implications for prompt NO formation](#)

J. Chem. Phys. **126**, 114311 (2007); 10.1063/1.2710271

[Atom-radical reaction dynamics of \$O\(3P\) + C_3H_5 \rightarrow C_3H_4 + OH\$: Nascent rovibrational state distributions of product OH](#)

J. Chem. Phys. **117**, 2017 (2002); 10.1063/1.1486441

[C–Cl bond fission, HCl elimination, and secondary radical decomposition in the 193 nm photodissociation of allyl chloride](#)

J. Chem. Phys. **116**, 2763 (2002); 10.1063/1.1433965

[Kinetics and dynamics in the photodissociation of the allyl radical](#)

J. Chem. Phys. **107**, 3329 (1997); 10.1063/1.474704

[Fast beam photodissociation spectroscopy and dynamics of the vinoxy radical](#)

J. Chem. Phys. **106**, 3049 (1997); 10.1063/1.473419



Photodissociation dynamics of the allyl radical

Hans-Jürgen Deyerl, Ingo Fischer,^{a)} and Peter Chen^{a)}

Laboratorium für Organische Chemie der ETH Zürich, Universitätstrasse 16, CH-8092 Zürich, Switzerland

(Received 31 August 1998; accepted 15 October 1998)

The photochemistry and photodissociation dynamics of the allyl radical upon ultraviolet (UV) excitation is investigated in a molecular beam by using time- and frequency-resolved photoionization of hydrogen atoms with Lyman- α -radiation. The UV states of allyl decay by internal conversion to the ground state, forming vibrationally hot radicals that lose hydrogen atoms on a nanosecond time scale. Two channels are identified, formation of allene directly from allyl, and isomerization from allyl to 2-propenyl, with a subsequent hydrogen loss, resulting in both allene and propyne formation. The branching ratio is between 2:1 and 3:1, with direct formation of allene being the dominant reaction channel. This channel is associated with site-selective loss of hydrogen from the central carbon atom, as observed in experiments on isotopically labeled radicals. *Ab initio* calculations of the reaction pathways and Rice–Ramsperger–Kassel–Marcus (RRKM) calculations of the rates are in agreement with the mechanism and branching ratios. From the measured Doppler profiles a translational energy release of 14 ± 1 kcal/mol is calculated. The calculated value of 66 kcal/mol for the barrier to the 1,2 hydrogen shift from allyl radical to 2-propenyl is confirmed by the experimental data. © 1999 American Institute of Physics. [S0021-9606(99)01003-X]

I. INTRODUCTION

A detailed understanding of the chemical reactions of organic radicals is often crucial for a realistic description of complex chemical systems where they appear as reactive intermediates. This requires the identification of the products formed in the reactions of these radicals, as well as a determination of the reaction rates and the energetics, i.e., the distribution of the excess energy into the product degrees of freedom. Whenever thermochemistry permits the appearance of several products, the relative rates for each reaction channel become important and branching ratios have to be determined. As the reactivity of any molecule depends on the internal energy deposited in the system, experiments are best carried out at well defined excitation energies.

The radical we currently investigate is the allyl radical, C_3H_5 , an important intermediate in combustion processes^{1,2} and possibly in tropospheric chemistry. It is a relatively stable radical that becomes reactive upon photochemical excitation. The 2A_2 ground state was thoroughly investigated by high-resolution infrared (IR) spectroscopy, allowing an accurate determination of the ground-state geometry.^{3,4} While relatively little is known about the structure of the lowest electronically excited 2B_1 state,⁵ starting to absorb around 400 nm, there is considerable information on the UV band system to the blue of 250 nm. Several vibronic bands were investigated by multiphonon-ionization (MPI) spectroscopy^{6–10} and assigned to the B^2A_1 , C^2B_1 , and D^2B_2 states, which are strongly coupled to each other. Geometries for these states were derived from partially rotationally resolved MPI spectra.^{9,10}

Recently we started to investigate the dynamics of the allyl radical upon photochemical excitation into the UV band

system, with the aim of identifying the reaction products as well as their energetics and the rate of formation.¹¹ The chemistry of the allyl system is rather complex because several reaction channels are thermochemically accessible upon excitation to the UV bands at an energy of 4.996 eV, corresponding to 115 kcal/mol. Six important reaction channels are summarized in Fig. 1, with the heats of formation taken from the literature.^{12–14} Three of them, formation of the C_3H_4 species cyclopropene, allene, and propyne, are associated with loss of a hydrogen atom, an enthalpically and entropically favorable reaction for radicals, because a closed shell species is formed and the reverse barriers for atom–molecule reactions are low. Two more channels, yielding cyclopropenylidene and propargyl, are associated with the loss of H_2 . Although formation of both C_3H_3 isomers is close in energy to the other channels, the loss of a hydrogen molecule is expected to proceed via a high activation barrier and is thus not considered in this study. Note that a sequential loss of two hydrogen atoms is thermochemically not possible at excitation energies around 5 eV. In principle, a reaction yielding acetylene and a methyl radical would also be thermochemically possible as the products are only higher in energy by 49 kcal/mol. However, this reaction requires two subsequent 1,2 hydrogen shifts before the C–C bond breakage. As will be shown below, the reaction is kinetically disfavored in comparison to hydrogen loss and can be neglected at the excess energies present in our experiments.

While a recently submitted paper gives a full account on the early time dynamics of the system, i.e., the nonradiative decay of the UV bands,¹⁵ we will here focus on the reactions occurring from the hot ground-state molecules. Detection of hydrogen atoms by resonant MPI [or, alternatively, by laser induced fluorescence (LIF)] is well suited for that investigation, first because H loss is an important reaction channel for radicals, and second, because of the very large cross section

^{a)}Authors to whom correspondence should be addressed.

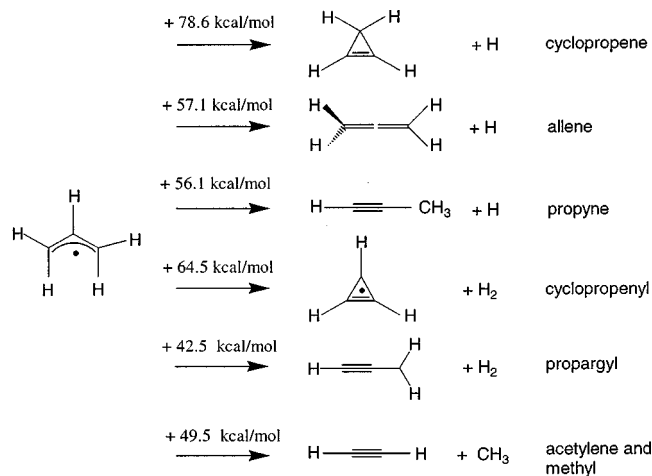


FIG. 1. The possible reaction channels thermochemically accessible for the allyl radical at an energy of 115 kcal/mol, corresponding to excitation of the C-state origin at 248.15 nm. The last three channels leading to the C_3H_3 isomers propargyl and cyclopropenylidene and molecular hydrogen, or acetylene and methyl, respectively, are expected to proceed via high activation barriers and thus to be irrelevant at the excess energies present in the system.

for the $1s-2p$ transition in atomic hydrogen at 121.6 nm (Lyman- α), which makes H-atom detection an extremely sensitive technique. The product appearance time can be obtained from time-resolved detection of the H atoms, giving microcanonical rates for product formation. Information on the energetics of the reaction can be gained from an analysis of the Doppler broadening in the hydrogen spectrum, which can be detected with commercially available standard dye lasers, due to the low mass of hydrogen. The application of the technique to chemical problems was pioneered in the 1980's by the groups of Welge,¹⁶ Kleinermanns and Wolfrum,¹⁷ Bersohn,^{18,19} and Wittig,²⁰ and is by now widely applied in experiments on elementary reaction dynamics.²¹ While the majority of experiments was carried out in cells, with hydrogen detection performed via LIF, some experiments in molecular beams were also reported.^{16,20,22} However, most of the work dealt with stable molecules.

As shown before by our group, a clean beam of radicals with relatively large number densities can be generated by supersonic jet flash pyrolysis,^{12,23} providing a way around the problems associated with photolysis, like interfering multiphoton transitions. As we demonstrated in our earlier communication,¹¹ the combination of pyrolytic generation of radicals with the detection of hydrogen atoms yields considerable insight into the chemistry of hydrocarbon radicals.

In addition to the work discussed in our earlier communication, we investigated the site specificity of the hydrogen loss by experiments on isotopically labeled compounds, 2-deuteroallyl and 1,1,3,3-tetradeuterioallyl, in order to gain more insight into the mechanism of the radicals' unimolecular decomposition. It can be assumed that allene formation will be associated with the loss of the central hydrogen atom in the 2-position, while cyclopropene formation should result in the loss of one of the terminal hydrogen atoms.

II. EXPERIMENT

The experiments were carried out in a standard molecular beam apparatus, equipped with a 1 m time-of-flight mass spectrometer. A clean beam of allyl radicals was generated by expanding allyl iodide, obtained from Aldrich, seeded in 1.5 bar of helium through a heated nozzle, mounted onto a pulsed General Valve with a 0.8 mm orifice. The radical concentration obtained with this technique at the nozzle exit is estimated to be on the order of 10^{14} cm^{-3} . The details of the design of our supersonic jet flash pyrolysis source were given in an earlier publication.²⁴ The beam passes through a skimmer into the main chamber, where it is crossed by two counterpropagating laser beams: one for excitation of the allyl radical (pump), and one for the detection of the hydrogen atoms (probe). We estimate a radical concentration of 10^{10} cm^{-3} in the ionization region. Typical operating pressures were on the order of several 10^{-6} Torr in the ionization region and 1×10^{-6} Torr in the flight tube.

In most experiments described here, two dye lasers (Quanta Ray PDL 2) pumped independently by injection-seeded Nd:YAG lasers (Quanta Ray GCR 3 and GCR 250) were employed, but in several later experiments an optical parametric oscillator (Spectra Physics MOPO 730) excited the allyl radical and induced photolysis. In most experiments the excitation laser was not focused. A digital delay generator (Stanford Research DG 535) controlled the relative timing between the two laser pulses to an accuracy within better than 2 ns, limited by the internal dither of the Nd:YAG lasers. The detection of hydrogen atoms was carried out via resonant MPI following the approach originally developed by the Welge group.²⁵ The output of a dye laser, operated around 365 nm, was focused by a 150 mm lens into a cell filled with 225 mbar of krypton in order to produce VUV radiation around 121.6 nm. The VUV light was focused into the ionization region by a 75 mm MgF_2 lens at the exit of the cell. Absorption of this wavelength excites hydrogen atoms from the 2S to the 2P state, which is located almost exactly at 3/4 of the ionization potential. Thus the residual fundamental suffices to ionize the excited hydrogen atoms that are detected in a time-of-flight mass spectrometer equipped with a dual stage Chevron-type microchannelplate detector. As the spectrometer was operated at a static field of 700 V/cm, H atoms excited into Rydberg states slightly below the ionization threshold were field-ionized under our experimental conditions. The signals were recorded in a digital storage oscilloscope, averaged over typically 200 shots, and transferred to a computer.

Three types of experiments were performed: (1) The excitation laser was scanned in frequency with the detection laser fixed at the Lyman- α -wavelength in order to record resonant MPI spectra of allyl and action spectra of hydrogen, (2) the excitation laser was fixed to a UV transition of the allyl radical, while the detection laser was scanned across the hydrogen or deuterium absorption band in order to record Doppler profiles of the atomic reaction product, and (3) both lasers were kept at a fixed frequency while the relative timing between the two was changed, i.e., a time-resolved pump-probe spectrum was recorded. The type (1) and (2) experiments were carried out at different delay times.

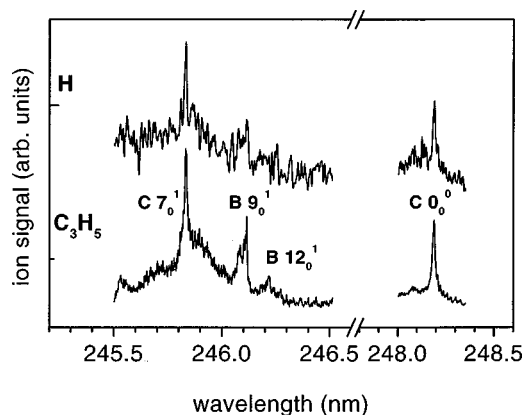


FIG. 2. The resonant MPI spectrum of allyl (lower trace) and the action spectrum of hydrogen atoms (upper trace), recorded simultaneously as a function of excitation wavelength. As visible, each resonance in the allyl spectrum is associated with a corresponding increase in the hydrogen signal.

III. RESULTS

A. C_3H_5

The results in this section were the subject of our preliminary report.¹¹ In a first experiment, the excitation laser was scanned around the C -state origin at 248.15 nm and through the UV band from 246.5 to 245.5 nm with the probe laser fixed at the Lyman- α wavelength. The signal in both mass channels, $m/e=41$ (allyl) and 1 (hydrogen), was recorded in parallel as a function of the excitation wavelength at a time delay of 100 ns between the laser pulses. From the resulting MPI spectrum depicted in Fig. 2, it is evident that for each peak in the allyl channel a corresponding peak appears in the hydrogen channel. The transitions into the $C 0_0^0$, $C 7_0^1$, and $B 9_0^1$ are visible, while the hydrogen signal associated with the $B 12_0^1$ band is somewhat obscured by the smaller signal-to-noise ratio (S/N). To decide whether a hydrogen is lost from the neutral radical or from the allyl cation, we measured the signal's power dependence, shown in Fig. 3 for the $C 7_0^1$ band. As can be seen, the magnitude of the hydrogen signal (open diamonds, full line) depends linearly on the excitation laser power, as expected for hydrogen

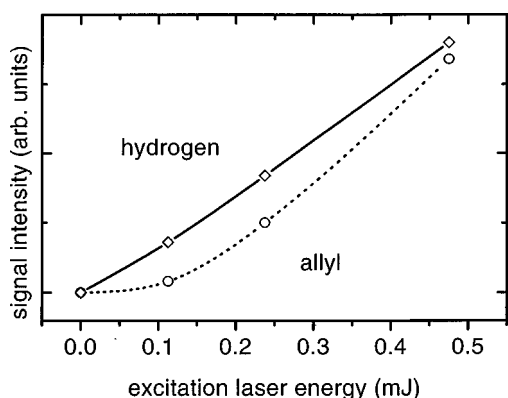


FIG. 3. Dependence of the signal on the pulse energy of the excitation laser. The hydrogen signal (open diamonds, full line) increases linearly with the pulse energy, as expected for H loss from neutral allyl radicals, while the allyl signal (open circles, dotted line) shows an approximately quadratic dependence.

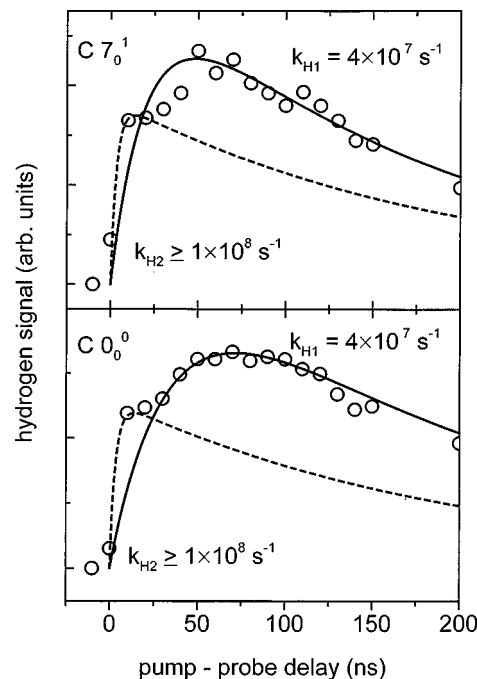


FIG. 4. Appearance of the hydrogen signal as a function of time delay between excitation laser and Lyman- α laser for initial excitation into the $C 0_0^0$ (lower trace) and $C 7_0^1$ state (upper trace). The solid line represents an exponential fit, employing a rate constant of $4 \times 10^7 \text{ s}^{-1}$. As the H atom is moving out of the line of sight, the signal decays at longer delay times. Note the deviation of the earliest data point at 10 ns from the fit in both traces, indicating the presence of a second process with a rate of approximately $1 \times 10^8 \text{ s}^{-1}$, drawn as a dashed line.

loss in the neutral. For comparison, the power dependence of the allyl signal (open circles, dotted line) is also given in the plot. It is well represented by a quadratic function, as it should be for two-photon ionization, indicating that saturation is not important under our conditions. Thus we conclude that hydrogen is indeed lost from neutral allyl radicals. Fast hydrogen atoms, originating from fragmentation in the ion, were observed at very high excitation laser intensities. They showed a different time dependence as well as an anisotropic Doppler profile, and could thus be easily distinguished from the hydrogen atoms originating from the neutral. No hydrogen was detected when the probe laser was blocked. The probe laser alone did produce a small hydrogen signal (5%) due to VUV photodissociation or detection of hydrogen atoms formed in the pyrolysis source. In all data presented below this background was subtracted. In the following sections we will predominately discuss results obtained for the $C 0_0^0$ state, because of its superior S/N ratio, but data on the $C 7_0^1$ state are also given for comparison.

In order to obtain microcanonical rates for the hydrogen loss, the H-atom signal was monitored as a function of the time delay between the excitation and the detection laser. Figure 4 shows time-delay scans for excitation of allyl into the $C 0_0^0$ (lower trace) and $C 7_0^1$ (upper trace) vibronic states. Both curves show a fast rise on the ns time scale and a slow decay that is due to the hydrogen moving out of the detection region, and which does not have any physical meaning. As discussed elsewhere, the initially excited UV states decay within 20 ps or less,^{15,26} in agreement with the absence of

fluorescence reported earlier. Thus we conclude that hydrogen is not lost directly from the initially excited UV states, but rather from hot ground-state molecules produced by fast internal conversion of the initially excited states. The hot ground-state allyl subsequently dissociates on a ns time scale into C_3H_4+H . Following Bersohn,²⁷ the curves were fitted by the expression

$$S_{H1,2}(t) = N[\exp(-k_2t) - \exp(-k_{H1,2}t)], \quad (1)$$

with $S_{H1,2}(t)$ being the atomic hydrogen signal, $k_{H1,2}$ the unimolecular rate constant for hydrogen loss from allyl, and k_2 accounting for the decay of the signal. From this expression we derived a rate constant of $k_{H1} = 4 \times 10^7 \text{ s}^{-1}$ for initial excitation into the $C 0_0^0$ state. The resulting fit is depicted as a solid line in Fig. 4, and also fits the $C 7_0^1$ state, given in the upper trace, well. Note that the signal-to-noise ratio is significantly better for the $C 0_0^0$ state, as shown in the excitation scan, Fig. 2. Since the excess energy available for the reaction is different for all initially excited UV states, the reaction should become faster with increasing excitation energy. However, this difference is too small to be observed in our experiments. The time scale for dissociation is long enough to assume complete randomization of energy, permitting us to treat the data within the framework of statistical theories. Interestingly, in both curves there appears reproducibly an early data point at around 10 ns, which does not fall onto the fitting curve. Although one might be tempted to regard the deviation of this point from the fit to be within the experimental error bars, we believe, in light of our work described in the latter sections, that this deviation is real. We interpret it as being due to the existence of two different reaction channels, as will be discussed below, and assign a tentative rate of $k_{H2} = 1 \times 10^8 \text{ s}^{-1}$ to it (dashed line).

In the dissociation process, part of the excess energy will be released as translational energy. Conservation of momentum requires that most of the translational energy will be carried away by the hydrogen atom, leading to a Doppler broadening of the absorption line. From the Doppler profile, information on the dissociation mechanism can be obtained. In a rapid dissociation process there is no time to redistribute the excess energy between the internal degrees of freedom, leading to a large, but anisotropic translational energy release and structured Doppler profiles. On the other hand, a complete redistribution of the internal energy before the dissociation, as required for the application of statistical theories, will lead to an isotropic energy distribution and unstructured Doppler profiles that are peaked in the center and can be approximately described by a Gaussian. In Fig. 5, Doppler profiles recorded for H atoms originating from initial excitation into the $C 0_0^0$ (lower trace) and $C 7_0^1$ (upper trace) are given, which can both be well fitted by a Gaussian with a full width at half maximum (FWHM) of 4.1 cm^{-1} , in agreement with a statistical dissociation process. (We are aware that a Gaussian Doppler profile is in itself not sufficient proof of statistical behavior.)

From the half-width of the Doppler profile, a translational temperature can be derived via the expression

$$\delta\omega_D = (\omega_0/c) \sqrt{8kT \ln 2/m_H}, \quad (2)$$

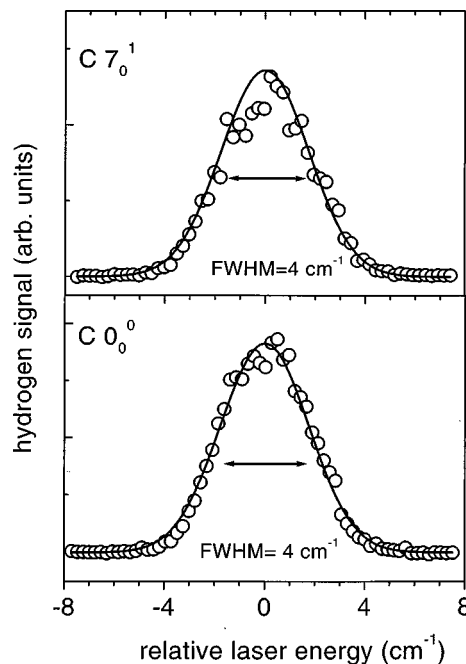


FIG. 5. H-atom Doppler profiles after excitation into the $C 0_0^0$ (lower trace) and $C 7_0^1$ state (upper trace). A Gaussian fit (full line) yields an expectation value of $14 \pm 1 \text{ kcal/mol}$ for the translational energy release.

from which we obtain the translational energy $E_{\text{trans}} = 3/2 kT$. This approach implicitly assumes a Boltzmann-like distribution of E_{trans} . In principle, the Doppler profile of hydrogen consists of two fine structure lines due to the $j = 1/2$ and $j = 3/2$ states, separated by 0.4 cm^{-1} , that are both broadened by the laser linewidth of 0.5 cm^{-1} , requiring a proper deconvolution. Experiments on a beam of H atoms produced from H_2 at a hot filament resulted in a Gaussian Doppler profile with a FWHM of 1 cm^{-1} . Employing this value in the deconvolution we arrive at a linewidth of 4.0 cm^{-1} , corresponding to a translational temperature of roughly 4600 K and an expectation value for the translational energy release of $14 \pm 1 \text{ kcal/mol}$, if an uncertainty of 0.1 cm^{-1} for the determination of the FWHM is taken into account.

If allene were the reaction product, 24% of the excess energy of around 59 kcal/mol would be released as translation. For propyne formation a similar value of 23% is calculated, while cyclopropene formation would be associated with 37% of the excess energy being released as translation. Typically, for hydrogen loss from unsaturated hydrocarbons, translational energy releases between 10% and 20% of the excess energy have been reported.^{18,19,27} The values determined for allene and propyne formation are within this range, although at the upper limit, the value for cyclopropene formation is clearly outside the range expected for this type of reaction.

While the expectation value for the translational energy release can be obtained from such a simple analysis of a Doppler profile, one is often interested in the details that a knowledge of the complete distribution of the translational energy provides. In an ideal case, the product translational energy distribution can be calculated by utilizing simple

models, like the prior distribution approach²⁸ or RRKM calculations,^{29,30} assuming that the energy in the reaction coordinate is released as translation. In either case, the distribution $P(E_{\text{trans}})$ is proportional to $E_{\text{trans}}^{1/2}$, yielding an expectation value of ≈ 7 kcal/mol, significantly less than the experimental value determined from the Doppler profile. However, this simple model does not take the energy of the reverse activation barrier into account, restricting its applicability to reactions with a loose transition state. As we have calculated reverse barriers of several kcal/mol for all reaction pathways (see below), those approaches are inappropriate. More recent models^{31,32} deal with the reverse barrier by dividing the total energy available to the products into two reservoirs, the statistical reservoir, defined as the difference between the total energy and the zero-point energy of the transition state, and a so-called impulsive reservoir that contains the energy difference between the zero-point energy of the product and the transition state, i.e., the reverse activation barrier. For the latter, one assumes that the distribution onto the different product degrees of freedom can be treated by the impulsive model^{33,34} which is in general used for the description of direct dissociation processes. Typically, in the impulsive model most of the energy is released as translation. For several examples, correct expectation values for the translational energy release were calculated this way.^{31,32} As shown below, in the case of allyl, the large Doppler shift can also be explained by assuming that most of the reverse activation barrier is released as translation. However, the treatment of the reverse barrier in the framework of the impulsive model leads to flat top Doppler profiles, indicating that this model does not describe the physics of the dissociation process properly.

B. Isotopically labeled compounds

Substituting hydrogen with deuterium allows for an investigation of the site selectivity of the reaction. For a dissociation forming allene, one would expect a loss of the hydrogen atom connected to the central carbon in allyl. Upon cyclization, on the other hand, one of the terminal C–H bonds should be cleaved. And finally, propyne formation, requiring a 1,2 hydrogen shift, might give rise to isotopic scrambling. Probing the site specificity of the reaction by partially deuterating the parent molecule in either the central or all terminal positions should thus aid the identification of the reaction products. The $1s$ - $2p$ Lyman- α transition in D is blue shifted only by 22.4 cm^{-1} with respect to H, so a Doppler profile can be recorded in a very similar manner. Due to the closeness of the two transitions we assume that the number of VUV photons produced in the tripling process is constant over the whole range. Assuming, in addition, that the absorption and ionization cross sections for H and D are similar, we can compare the area under the hydrogen and deuterium peaks in the spectra without any further correction and assume that they are directly proportional to the relative number of H and D lost from the parent at a given time. Although there are examples for isotopic scrambling obscur-

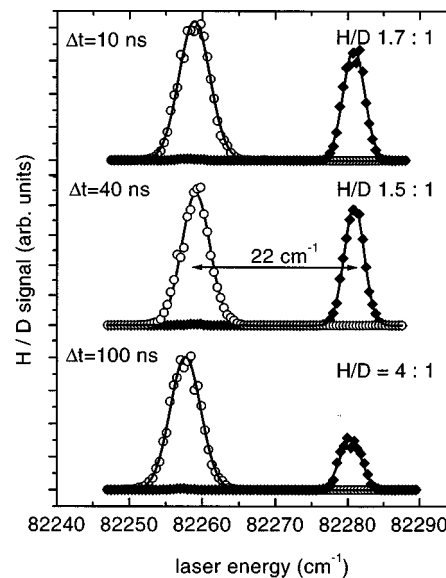


FIG. 6. Doppler profiles for the 2-deuterioallyl at different time delays. The H signal is given by open circles, the D signal by full diamonds. The solid line constitutes a Gaussian fit. At early times there is a clear preference for deuterium loss in the dissociation, but interestingly the relative ratios between H and D change with time.

ing any selectivity,³⁵ there are also cases of unimolecular dissociations, where such site specificity has been observed.³⁵

However, one has to consider that in experiments on isotopically labeled compounds, a regular kinetic isotope effect will be present.³⁶ Replacement of hydrogen with deuterium will change the zero-point energies as well as the density of states, due to the lower frequency of $-X-D$ as compared to $-X-H$ vibrations. As a result, reaction rates will in general decrease upon deuteration of the C–H bond that is broken.

For the isotopically labeled compounds, neither excitation and action spectra nor power dependencies were recorded, due to the small amount of substance available. As the NMR spectra of the labeled compounds³⁷ indicated the presence of CH_3I and $(\text{CH}_3)_3\text{SiOH}$, we ensured that neither of the two contaminants gave rise to hydrogen signals under our conditions. The labeled species were excited to the $C 0_0^0$ band¹⁰ at 248.22 (monodeuterated) and 248.21 nm (tetradeuterated) under conditions similar to those employed in the C_3H_5 experiments.

Three such Doppler scans for the monodeuterated allyl radical, recorded at pump–probe delay times of 10, 40, and 100 ns are presented in Fig. 6, together with the relative ratio of hydrogen (open circles) and deuterium (full diamonds), as obtained from the integral under the Gaussian used to fit the Doppler profiles. The H/D ratio is around 1.7:1 at the early delay times and reaches 4:1 at a delay of 100 ns. Note that it is not possible to measure the relative ratio at substantially longer delay times, because the hydrogen atoms leave the observation region faster than the deuterium atoms. The width of the Doppler profiles is considerably smaller for deuterium because of its $m^{-1/2}$ dependence. The FWHM of 2.8 cm^{-1} after deconvolution yields the same translational energy release of 14 kcal/mol as for the hydrogen atoms, how-

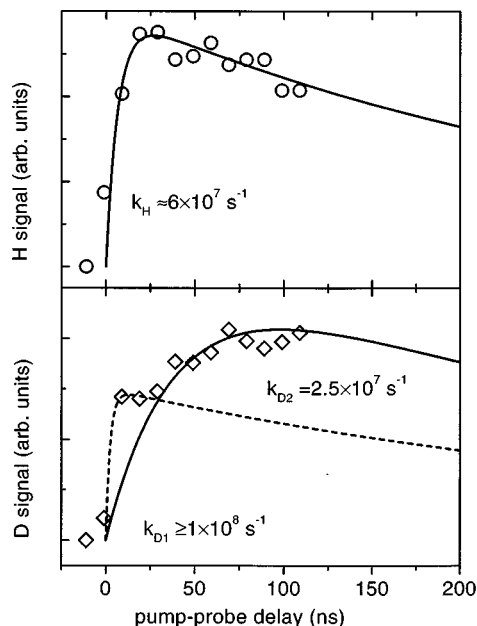


FIG. 7. Rates for H (upper trace, open circles) and D loss (lower trace, open diamonds) from 2-deuterioallyl. There are two rates present in the D-loss channel, in agreement with the change in H/D ratio as observed in the Doppler profiles, Fig. 6.

ever, with slightly larger error bars. Using similar arguments as before, they are in good agreement with allene and propyne formation, but not with cyclopropene formation.

Two interesting results are apparent from the scans given in Fig. 6: first, deuterium is lost more rapidly than hydrogen. This is in contrast to the expected kinetic isotope effect and thus indicates a preference for allene formation. Second, the relative ratio between H and D changes with time. In order to obtain a change in the relative ratio with time, two different species have to be involved, because a loss of H and D from the same precursor would yield a time-independent ratio. Thus only the assumption of two different reaction channels originating from two different, but chemically related, species can explain the change in relative intensity of the Doppler profiles.

Another striking feature is the almost constant H/D ratio at 10 and 40 ns. If one records the H (upper trace) and D (lower trace) signal, respectively, as a function of the pump-probe delay, the curves given in Fig. 7 are obtained. Interestingly, there is a plateau at 40 ns in the graph describing deuterium formation, in agreement with the constant H/D ratio at 10 and 40 ns, and resembling the early data points in the time-delay scans for the fully hydrogenated compound in Fig. 4. We can thus extract two rate constants from the time delay scan, $k_{D1} \geq 1 \times 10^8 \text{ s}^{-1}$ for the faster process, and $k_{D2} = 2.5 \times 10^7 \text{ s}^{-1}$ for the slower one. Hydrogen loss, on the other hand, can be described well by a smooth curve with a rate constant $k_H = 6 \times 10^7 \text{ s}^{-1}$, indicating the existence of two channels for deuterium formation and one channel for hydrogen formation.

In order to check for internal consistency, the same experiments were conducted on the isotopic mirror image, C_3HD_4 , with the hydrogen attached to the central carbon atom. The resulting Doppler profiles are given in Fig. 8.

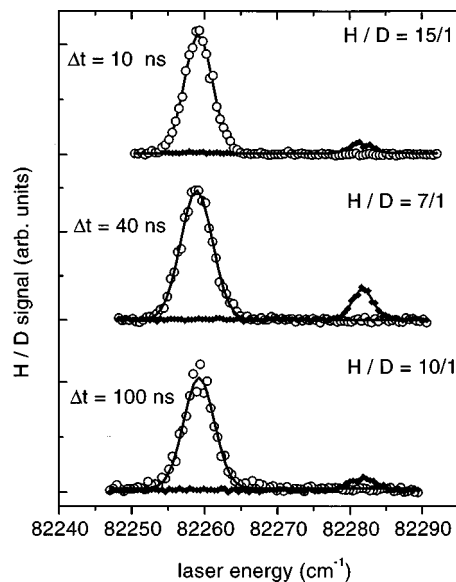


FIG. 8. Doppler profiles for tetra-deuterioallyl at different time delays, demonstrating the preference for H loss, and thus allene formation. The H signal is again given by open circles, the D signal by full diamonds. The solid line constitutes a Gaussian fit.

Although there is only a single hydrogen present in the molecules, the spectrum at 10 ns is clearly dominated by the hydrogen signal, the H/D ratio being 15:1. At later delay times the relative ratio decreases, but hydrogen loss is still the dominating process. Interestingly, the relative amount of deuterium is largest at 40 ns (H/D=7:1), but decreases again, reaching H/D=10:1 at 100 ns delay.

Again we recorded time-delay scans in order to get access to the rates for the processes, which are given in Fig. 9.

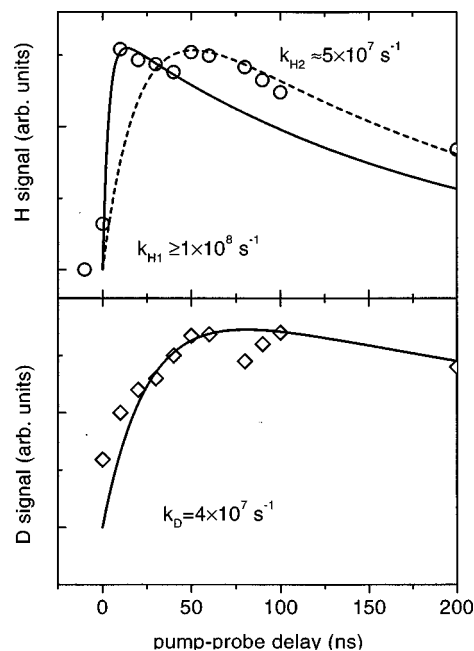


FIG. 9. Rates for H (upper trace) and D loss (lower trace) from tetra-deuterioallyl. This time there are two rates present in the H-loss channel. Due to the small amount of D loss (see Fig. 8) the signal-to-noise ratio in the D channel is rather poor.

The curve for hydrogen loss (upper trace), showing a very fast rise with a maximum at 10 ns, followed by a slight decrease and a second rise, is again in agreement with the picture developed above, a loss channel directly from allyl, and a second channel via a high energy intermediate. We can derive rate constants $k_{H1} \geq 1 \times 10^8 \text{ s}^{-1}$ and $k_{H2} = 5 \times 10^7 \text{ s}^{-1}$. The curve for deuterium loss, given in the lower trace, is somewhat ambiguous due to the small overall signal magnitude and the subsequently higher signal-to-noise ratio. The solid line represents a tentative fit with a rate constant of $k_D = 4 \times 10^7 \text{ s}^{-1}$. We note that we had to restrict ourselves to a relatively small number of experiments because the isotopically labeled precursors were only available in small amounts. For that reason, the time-delay scans given in Figs. 7 and 9 were not reproduced.

The qualitative behavior is in agreement with the picture derived from the experiments on the monodeuterated compound. The H or D atom, respectively, that is connected to the central carbon atom, is lost faster than the atoms connected to the terminal carbons, indicating a preference for allene formation. For CD_2CHCD_2 , the intrinsic preference for cleavage at the 2-position is reinforced by the isotope effect, while for CH_2CDCH_2 , the two effects work in opposite directions.

C. Electronic structure calculations

To aid the analysis of our experimental data, *ab initio* calculations were performed, using the GAUSSIAN 94 program package.³⁸ The main goal was the calculation of data necessary for a statistical analysis, in particular reliable vibrational frequencies for the transition states of the different reaction channels and activation barriers, which are both needed for RRKM calculations. In a first step, we performed a geometry optimization by fourth-order perturbation theory (MP4) including single, double, and quadruple excitations, employing a 6-31 G* basis set. These calculations yielded a good description of the reaction path for all channels, including the geometries for the transition states. Subsequently, a vibrational frequency analysis was performed at all stationary points on the MP4 level. By comparing the frequencies calculated for the allyl radical with the experimentally determined values,^{39,40} a scaling factor of 0.945 was derived, which was employed for the transition state frequencies as well.

In order to achieve high accuracy in the determination of the activation barriers, we performed single point CCSD(T) coupled cluster calculations at the geometries optimized at the MP4 level for the stationary points (educt, transition state, and product) for every reaction channel. Here we employed the correlation consistent valence triple zeta basis set (cc-pVTZ),⁴¹ which consists of a $(10s5p2d1f) \times [4s3p2d1f]$ contraction on each carbon atom and a $[3s2p1d]$ contraction on each hydrogen. While the carbon 1s orbitals were frozen on the UHF level, all other electrons were included in the calculation of the correlation energy. The details of all calculations can be obtained from the supplementary material.³⁷

The energetics for the reaction pathways leading to allene and cyclopropene are given in Fig. 10. A 1,2 hydrogen

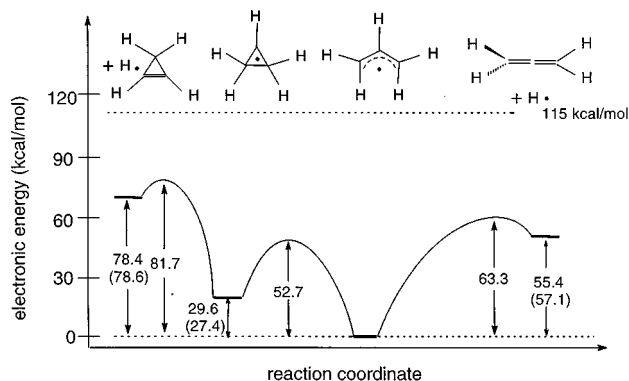


FIG. 10. Computed reaction coordinate for the pathways leading from allyl to cyclopropene (left-hand side) and allene (right-hand side). The values in brackets represent the experimentally known heats of formation for the reaction products.

shift, leading to the 2-propenyl radical, constitutes an alternative pathway, depicted in Fig. 11. Hydrogen loss from 2-propenyl can either lead to the formation of propyne (lower trace) or allene (upper trace). All energies are relative with respect to the electronic energy of the allyl radical, which was chosen as the reference point. The calculated energies are zero-point corrected, using the calculated frequen-

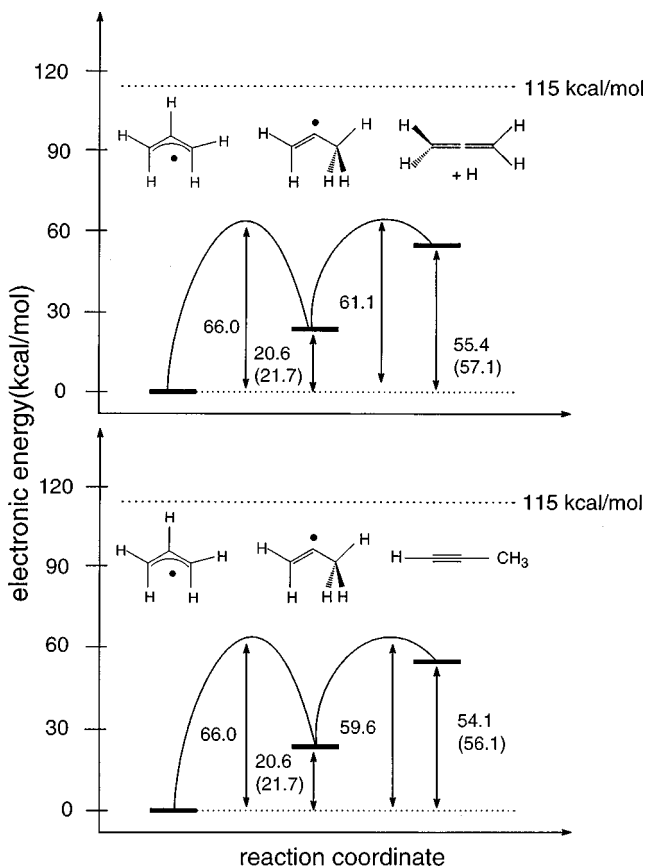


FIG. 11. Computed reaction coordinate for the pathways proceeding via the 2-propenyl intermediate. The barrier for the 1,2, hydrogen shift is comparable to the barrier to allene formation. From 2-propenyl, two product channels are accessible, propyne (lower trace) and allene (upper trace). The calculations indicate that propyne should be preferentially formed from methylvinyl due to the lower barrier. All electronic energies given in the figure are zero-point corrected.

cies multiplied by 0.945. The experimental values for H_f are given in brackets below the calculated electronic energies whenever they are known.^{12,13} They agree within ± 2 kcal/mol with the *ab initio* electronic energies. In calculations of activation barriers it is very hard to obtain chemical accuracy, so it is reasonable to assume at least the same error bars. For the reaction yielding allene, we calculated a reverse barrier of 7.9 kcal/mol, resulting in a total activation barrier of 63.3 kcal/mol. Assuming that most of the energy in the reverse barrier is released as translation in the reaction, we can thus, in principle, account completely for the 6–8 kcal/mol difference between the observed expectation value for the translational energy release of 14 and the 7 kcal/mol obtained from RRKM calculations or a prior distribution approach. The reaction to cyclopropene proceeds via the cyclopropyl radical that is only 27 kcal/mol higher in energy than allyl itself. The activation barrier of 52.7 kcal/mol for cyclization is in good agreement with both earlier calculations⁴² and the experimental value of 49.4 kcal/mol.⁴³ However, the barrier to cyclopropene formation is almost 82 kcal/mol, the highest of all channels investigated. We also calculated the barrier to 1,2 hydrogen shift within the cyclopropyl radical, which is as high as 75 kcal/mol relative to allyl, and thus unimportant under our conditions. On the other hand, a barrier of 66.0 kcal/mol was calculated for isomerization to 2-propenyl via a 1,2 hydrogen shift, only slightly higher than the barrier to allene formation. The calculated transition state geometry indicates an almost triangular configuration, the H-atom being in between the two carbon atoms. In conclusion, from the computations it can be expected that both pathways, allene formation from allyl and isomerization to 2-propenyl, are important.

We also calculated the pathway for a second consecutive 1,2 hydrogen shift within 2-propenyl, with one of the methylenic hydrogens moving to the central carbon. This leads to the 1-propenyl isomer, with the radical center located at the terminal carbon atom. We found an electronic energy of 24.6 kcal/mol relative to allyl for this radical, and a barrier of 68.3 kcal/mol for isomerization between the two propenyl isomers. Thus a second 1,2 H shift is unfavorable compared to dissociation. This also indicates that cleavage of the C–C bond into acetylene and methyl, a pathway that requires a sequence of two 1,2 H shifts and is expected to have a reverse barrier significantly higher than an atom–molecule reaction, is unlikely to occur under our conditions on kinetic grounds. However, at higher excess energies it might constitute an important reaction channel.

D. RRKM calculations

In order to calculate reaction rates for the different pathways, RRKM calculations were performed for all three reaction channels, allene, propyne, and cyclopropene formation. All rates presented below were obtained employing direct vibrational state count,⁴⁴ but a program utilizing the Whitten–Rabinovich algorithm³⁰ yielded identical results. All frequencies,³⁷ scaled by 0.945 in order to match the experimentally known frequencies of the allyl radical, and the reverse activation barriers were obtained from *ab initio* calculations as described above.

It was shown in electron spin resonance (ESR) experiments several years ago that the barrier to rotation around the C–C bond in the allyl radical is only 15.7 ± 1 kcal/mol.⁴⁵ Thus the methylene groups have to be regarded as free rotors at the high excess energies present in our experiment. Good agreement between experimental and calculated values was achieved when both of the torsional frequencies of 525 and 545 cm^{-1} were replaced in the RRKM calculations by 100 cm^{-1} . We did not correct the frequencies in the transition state, because the *ab initio* geometries did not indicate the presence of hindered rotors. The transition states for the major reaction channels were calculated to be of C_s symmetry or lower,³⁷ so a symmetry number of 2 was employed in the RRKM calculations.

Formation of allene by direct hydrogen loss from allyl, as depicted in Fig. 10, represents the ideal case of a unimolecular dissociation that can be described by a single rate constant. A rate of $4.2 \times 10^8 \text{ s}^{-1}$ was calculated, on the order of the experimentally observed value. Without correcting for the free internal rotation, i.e., employing torsional frequencies of 525 and 545 cm^{-1} , the rate constant became one order of magnitude faster.

As visible from Figs. 10 and 11, both cyclopropene and propyne formation are two-step processes via a high energy intermediate. In this situation, one of the basic assumptions of RRKM theory, that the rate depends only on the energy and not on the mechanism, becomes questionable. However, the situation simplifies considerably for the pathway leading to cyclopropene. Cyclization of allyl will yield in a first step a cyclopropyl radical with an activation barrier of 52.7 kcal/mol. At the energies present in the molecule, cyclopropyl loses an H atom to form cyclopropene, via a transition state that lies about 82 kcal/mol above the ground state of allyl. Thus at the large amount of excess energy present in the system, the cyclization will be very rapid, so we can ignore the cyclopropyl intermediate and describe the overall process by a single rate constant, k_{cyc} . This is the well-known Curtin–Hammett principle. For the RRKM calculations of k_{cyc} , the density of states of the allyl radical was employed in the numerator, while the number of states at the transition state of the cyclopropyl–cyclopropene reaction appears in the denominator. A rate constant of $4 \times 10^6 \text{ s}^{-1}$ was calculated for cyclopropene formation, about two orders of magnitude slower than allene formation. This confirms that cyclopropene formation is not important under our conditions. Any allyl that ring closes ($k_{\text{close}} = 8 \times 10^8 \text{ s}^{-1}$) will ring open back to allyl again ($k_{\text{open}} = 1.4 \times 10^{10} \text{ s}^{-1}$) before it can lose an H atom.

For propyne formation, a reaction that proceeds via the 2-propenyl radical, the situation is more difficult. As depicted in the figures, the barrier to isomerization is comparable to the barrier to dissociation. Although strictly speaking the barrier to 2-propenyl constitutes a bottleneck in phase space that prevents the system from full equilibration before dissociation, we can try to treat it as a series of two unimolecular processes, an isomerization and a dissociation. To complicate matters further, the 2-propenyl route provides access to two products. Upon loss of a hydrogen atom at the CH_2 group, propyne is formed, whereas hydrogen loss from

the $-\text{CH}_3$ group in 2-propenyl will yield allene. As the barrier to allene formation was calculated to be ≈ 2 kcal/mol higher in energy than the barrier to propyne formation, the latter channel is expected to dominate. In any case, due to the higher barrier, the isomerization to 2-propenyl is the rate-determining step, calculated to be $1.9 \times 10^8 \text{ s}^{-1}$, while the hydrogen loss to propyne was calculated to be $3 \times 10^{11} \text{ s}^{-1}$. Thus the experimental rates give the rate for the isomerization. We also calculated a rate of $1.7 \times 10^{10} \text{ s}^{-1}$ for the reaction back to allyl. This means that less than one out of ten 2-propenyl radicals formed will react back to allyl instead of dissociating.

The RRKM calculations for the deuterated species yielded only a small rate decrease by typically a factor of 2 (primary) or less (secondary). For the reaction from allyl to allene a rate of $1.9 \times 10^8 \text{ s}^{-1}$ was calculated for D loss from $\text{C}_3\text{H}_4\text{D}$, compared to $4.2 \times 10^8 \text{ s}^{-1}$ for H loss from C_3H_5 . For H loss from $\text{C}_3\text{D}_4\text{H}$, the rate decrease was even smaller, from 4.2 to $3.8 \times 10^8 \text{ s}^{-1}$. Such small isotope effects are not uncommon for reactions carried out at high excess energies. In experiments on partially deuterated ethylenes, for example, kinetic isotope effects ranging from 1.1 to 2.4 were reported.¹⁹ For the 1,2 hydrogen shift in 1,1,3,3-tetradeuterioallyl, we calculated a rate of $1.7 \times 10^8 \text{ s}^{-1}$, slower by a factor of 2.3 as compared to direct formation of allene from this precursor, while for the 2-deuterioallyl the calculated rate of $1.1 \times 10^8 \text{ s}^{-1}$ was slower only by a factor of 1.6. This is in agreement with the measured Doppler profiles (see Figs. 6 and 8), which show a more pronounced site selectivity, i.e., preference for allene formation, in the case of 1,1,3,3-tetradeuterioallyl.

IV. DISCUSSION

The photochemistry of the allyl radical was already addressed in several earlier studies, but the results are still ambiguous. Matrix-isolated allyl radicals,⁴⁶ as well as substituted allyl radicals grafted onto a silica surface,⁴⁷ are reported to cyclize upon irradiation at 400 nm. Irradiation in matrices at 254 nm, on the other hand, produced a mixture of products,⁴⁸ including allene and propyne. The gas-phase resonance Raman spectrum³⁹ recorded at 225 nm showed enhancement for the ν_{12} CH_2 torsional mode, in agreement with a disrotatory isomerization to cyclopropyl radical. This isomerization process can be regarded as the first step in the formation of cyclopropene, because at the excitation energies employed, the internal energy that would be present in the cyclopropyl radical would suffice for dissociation. The cyclization process was also the subject of several computational studies,^{42,49,50} while the other reaction channels, to the best of our knowledge, were not yet investigated theoretically. The first examples of monitoring the dissociation of organic radicals via H-atom detection were reported by Koplitz and co-workers,^{35,51} who investigated the site specificity of hydrogen loss in alkyl radicals. As they generated their radicals by photolysis, multiphoton processes complicated the analysis of the data. In the work presented here, H-atom detection was combined with pyrolytic generation of radicals.

In two earlier communications on the photodissociation dynamics, we demonstrated that the dynamics upon UV excitation is governed by two different time scales. The initially prepared states decay nonradiatively within 20 ps or less, as shown by ps time-resolved photoelectron spectroscopy,^{15,26} forming hot ground-state molecules. The hot allyl subsequently loses a hydrogen atom on a nanosecond time scale, which was detected by resonant MPI spectroscopy.¹¹ We found a rate of $k(E) = 4 \times 10^7 \text{ s}^{-1}$ for the hydrogen loss and a translational energy release of 13.6 kcal/mol, and showed that a statistical analysis of the data is in agreement with allene being the dominant reaction channel, while cyclopropene formation is unlikely to be important. The data presented here indicate that propyne formation has to be considered as a reaction channel as well, because the measured rates and translational energy releases are in agreement with both allene and propyne, and the calculated activation barriers for both channels are comparable.

From a first qualitative analysis of the experiments on isotopically labeled allyl radicals, two conclusions can already be derived: (1) There is a clear preference for loss of the central hydrogen or deuterium atom, respectively. This channel is associated with allene being the molecular fragment. (2) The relative rates of hydrogen and deuterium formation change with time. Thus there has to be a second hydrogen loss reaction, originating from a chemically different molecule. If both loss channels would originate from allyl, the relative rate could not change with time, because a reaction that yields a certain branching ratio at early delay times will yield the same branching ratio at late delay times. On the other hand, an isomerization process that competes with dissociation, yielding a C_3H_5 isomer, which subsequently loses *both* hydrogen *and* deuterium atoms, could explain this time dependence. In the case of the monodeuterated CH_2CDCH_2 such a scenario would lead to two chemically distinct species, one losing only D atoms, the other one losing H and D atoms, and subsequently three rates, the fastest one being the selective loss of deuterium from allyl radicals, resulting in the formation of allene. The second slower channel should yield both hydrogen and deuterium.

In principle there are two isotopic species that might account for this second reaction channel, cyclopropyl radical and 2-propenyl. As discussed above, there is no indication of cyclopropene formation in our experiments, which would be expected if hydrogen loss from cyclopropyl constituted an important reaction channel. H loss from a 2-propenyl intermediate, on the other hand, could lead to allene and propyne formation, both being in agreement with the statistical analysis of the rates and the Doppler profiles of both hydrogen and deuterium. In addition, our *ab initio* calculations indicate that isomerization to 2-propenyl is energetically similar to direct allene formation, so a competition can be expected.

In light of the data obtained for the deuterated allyl, we can now explain the time delay scan obtained for C_3H_5 . We interpret it as a convolution of two rates, a fast process, site-selective loss of the central H atom yielding allene, in competition with an isomerization to 2-propenyl with a subsequent H loss leading either to propyne or allene. The early

data point visible in Fig. 4 that does not fall on the solid curve is due to the fast process. While the rate constant of $4 \times 10^7 \text{ s}^{-1}$ is assigned to 2-propenyl formation, the rate for allene formation is at the limit of the time resolution for our experiment and can only be estimated to be around $1 \times 10^8 \text{ s}^{-1}$ or faster.

From the computational results discussed above, the pathway via the 2-propenyl radical should lead predominantly to propyne formation, because of the 2 kcal/mol lower activation barrier as compared to allene formation. For 2-deuteroallyl, one would thus expect the shifted deuterium to become part of the methyl group in propyne, i.e., loss of a hydrogen atom from the methylene group in 2-propenyl and formation of HCCCH_2D . In addition, this reaction should be favored over deuterium loss because of the kinetic isotope effect. However, the presence of two rates in the D-loss channel is evident from both the time-delay scans given in Fig. 7, as well as the Doppler profiles given in Fig. 6. We thus have to find the origin of the second D-loss channel originating from the 2-propenyl intermediate.

There are several possible explanations for the loss of deuterium from 2-propenyl. The most likely reason for a difference between observed and calculated rates is an error in the activation barriers, because it is hard to calculate transition state energies to within better than ± 2 kcal/mol. To our mind the best explanation is that in contrast to the *ab initio* results, the barriers to allene and propyne formation are approximately equal in magnitude, so there is no preference for either product. As the isomerization is the rate-determining step, the two reactions cannot be distinguished in the case of a fully hydrogenated allyl, but they can for the deuterated radicals. Another explanation could be that the barrier for the 1,2 hydrogen shift is lower than calculated. In this case, a higher fraction of 2-propenyl would isomerize back to allyl and lead to partial isotopic scrambling. As will be discussed below, a significantly lower activation barrier would be incompatible with the experimental observations.

In principle, one could imagine that the dissociation of the 2-propenyl intermediate is so fast that the energy is not fully equilibrated, prohibiting the application of statistical theories for this step. Indeed, a rate of $3 \times 10^{11} \text{ s}^{-1}$ is calculated for the reaction from 2-propenyl to propyne, corresponding to a reaction time of 30 ps, which might be too short to ensure complete energy randomization. However, we prefer the first explanation, inaccuracies in the calculation of the barriers to hydrogen loss from 2-propenyl, since it permits one to explain all observations within the framework of statistical theories.

The experimental rate for hydrogen loss from the 2-propenyl isomer of $\text{C}_3\text{H}_4\text{D}$ should be similar to deuterium loss, because the rate-determining step is identical. Both should also be slightly slower than the isomerization rate in C_3H_5 . In looking at the hydrogen channel, we observe a small increase, from 4×10^7 to $6 \times 10^7 \text{ s}^{-1}$, looking at the deuterium channel we find the expected decrease to $2.5 \times 10^7 \text{ s}^{-1}$. To our mind, this difference gives an idea of the error bars in the experiments on the deuterated species.

For the 1,1,3,3-tetradeuterioallyl, the appearance of two different rates for hydrogen loss is understandable. Forma-

tion of propyne from the 2-propenyl intermediate is associated with deuterium loss, while allene formation can proceed via hydrogen loss and is thus amplified by the kinetic isotope effect. Assuming equal transition state energies for the reactions from 2-propenyl to propyne and allene, allene formation should now be favored, in agreement with the very small deuterium signals observed (see Figs. 8 and 9). The small signals and the correspondingly low signal-to-noise ratio make it difficult to extract reliable H/D ratios. Nevertheless, two rates are visible in the hydrogen channel, $k_{\text{H1}} \geq 1 \times 10^8 \text{ s}^{-1}$ (allene-formation) and $k_{\text{H2}} = 5 \times 10^7 \text{ s}^{-1}$ (reaction via 2-propenyl), different by approximately a factor of two. The rate for deuterium loss from 2-propenyl is around $k_{\text{D}} \approx 4 \times 10^7 \text{ s}^{-1}$, showing no significant kinetic isotope effect, as expected from the discussion above.

Another issue of interest is the experimental verification of the barrier to 1,2 hydrogen shift in an organic radical. A significantly lower barrier would lead to complete isotopic scrambling, inconsistent with the observation of any site selectivity. A significantly higher barrier, on the other hand, would reduce the rate to isomerization to such an extent that this reaction channel could not be observed. We calculated rates for the isomerization, varying the calculated barrier of 66.0 over a ± 3 kcal/mol range. A reduction to 63 kcal/mol brings the RRKM rate for isomerization up to $3.6 \times 10^8 \text{ s}^{-1}$, close to the rate for direct formation of allene. The two rates are even closer for the monodeuterated allyl, in contrast to the observed site selectivity. A barrier higher by 3 kcal/mol, on the other hand, leads to a rate decrease by a factor of two, which is outside the experimental error bars. Varying the barrier height within ± 1 kcal/mol of the *ab initio* value yields good agreement with the experimental rates for C_3H_5 as well as for the deuterated compounds. Thus we conclude that the calculated barrier for the 1,2 H shift is confirmed by the observed rates.

Isomerization of the reaction products might pose problems for the data interpretation. It was found that cyclopropene is an intermediate in the reaction from allene to propyne.⁵² However, the barriers of 68.4 and 64.1 kcal/mol found for the allene \rightarrow cyclopropene and propyne \rightarrow cyclopropene reaction, respectively, are not accessible in the experiments described here.

Figure 12 summarizes the results obtained from the analysis of the kinetics. When we compare the experimental rates, given above the arrow, with the RRKM values, given in brackets below the arrows, of $4.2 \times 10^8 \text{ s}^{-1}$ (allene formation) and $1.9 \times 10^7 \text{ s}^{-1}$ (2-propenyl formation), we realize that the calculated rates are on the same order of magnitude, but slightly faster, and that the relative ratios match quite well, yielding $k_{\text{rel}} = k_{\text{allene}}/k_{\text{propenyl}} = 2.3$ from the calculations and 2.5 from the experiment.

With the kinetic data we can now extract branching ratios. Considering the error bars of experiment and calculations, we assume that $k_{\text{rel}} \approx 2.5$, but not smaller than $k_{\text{rel}} = 2$. The upper limit is not well defined, because the accuracy in the determination of the fast rate is limited by the time resolution of our setup. The agreement between the measured and calculated ratios for $\text{C}_3\text{H}_4\text{D}$, however, seems to confirm this branching ratio. In addition, a significant frac-

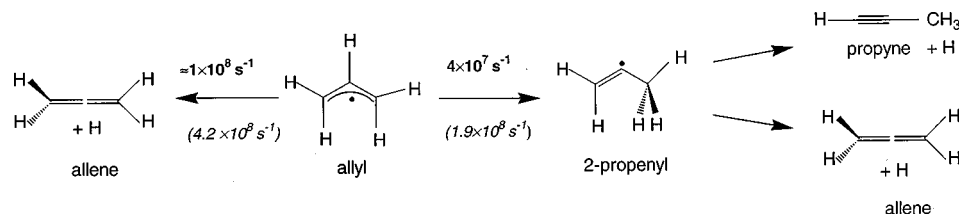


FIG. 12. Summary of the unimolecular chemistry of the allyl radical at 115 kcal/mol. Two competing pathways, formation of allene, and isomerization to 2-propenyl with subsequent hydrogen loss can be observed. The experimental rates, as well as the RRKM rates (italic, in brackets) are given in the figure. As visible, formation of allene is the faster, and thus dominating, channel.

tion of the 2-propenyl isomer will also dissociate into allene so that the overall product ratio allene/propyne is higher, probably between 3/1 and 4/1. Formation of cyclopropene or C–C bond cleavage to acetylene and methyl are considered to be of minor importance.

In applications there is often interest in the canonical rate constant, k_T , at a given temperature, rather than the microcanonical constant k_E . When the energy distribution is adequately described by a Boltzmann distribution, the relation becomes³⁴

$$k_T = Q^{-1} \int_{E=E_A}^{E=\infty} k_E \rho(E) e^{-E_i(kT)^{-1}} dE, \quad (3)$$

with Q^{-1} being the vibrational partition function and $\rho(E)$ being the density of states, corresponding to the degeneracy factor. We calculated k_T for the allyl→allene reaction for two temperatures, $T=4300$ K, the vibrational temperature of allyl, as derived before,¹¹ and $T=4600$ K, the observed translational temperature for the hydrogen atom, and obtained values of $k_{T=4300} = 9.5 \times 10^7$ and $k_{T=4600} = 9.6 \times 10^7$ s⁻¹. For the allyl→2-propenyl isomerization, we obtain $k_{T=4300} = 3.8 \times 10^7$ and $k_{T=4600} = 3.9 \times 10^7$ s⁻¹.

It is worthwhile to compare our approach to other techniques employed to study the dynamics of radicals. An interesting alternative is photofragment translational spectroscopy, developed by the Neumark group^{53–55} Here the radicals are produced by photodetachment in a fast beam of the corresponding mass selected anions. After excitation into dissociative or predissociative states by a tunable laser, the different fragments are detected in coincidence. This technique is general and provides a considerable amount of information; however, it is difficult to apply when the fragments are very different in mass, in particular when a hydrogen atom is lost. In addition, reaction rates can only be obtained indirectly. An extension of this technique was introduced by Continetti and co-workers, who detect the photoelectrons generated in the detachment step in coincidence with the neutral radicals or fragments.^{56,57} In contrast, Doppler spectroscopy, as applied by us, works best for small fragments. Thus both techniques complement each other very well.

V. CONCLUSION

In this paper we investigated the photochemistry and photodissociation dynamics of the allyl radical, C₃H₅, upon excitation into the UV bands to the blue of 250 nm. A clean and cold molecular beam of allyl radicals was generated by

supersonic jet flash pyrolysis of allyl iodide, C₃H₅I, seeded in helium. Action spectra showed that each UV resonance is associated with a hydrogen signal. The linear power dependence of the H signal on the excitation laser confirmed that hydrogen is lost from neutral allyl. Time-delay scans yielded an appearance time of several nanoseconds for the hydrogen atoms. Interestingly, they can be fitted best under the assumption of two processes with two different rates contributing to the signal. As picosecond lifetimes for the excited state were reported in earlier time-resolved experiments, we conclude that hydrogen is not lost from the excited states directly, but rather from the hot ground state, populated by internal conversion.

Partially deuterated precursors were employed in order to investigate the site selectivity of the hydrogen loss. Experiments on both C₃H₄D and C₃HD₄ showed a marked preference for hydrogen loss from the central carbon atom, resulting in allene formation being the major product channel. However, in addition, a second process was observed, that led to a change of the relative ratios between hydrogen and deuterium with delay time. This channel is assigned to isomerization to the 2-propenyl radical via a 1,2 hydrogen shift. 2-propenyl subsequently loses a hydrogen atom to form either allene or propyne. *Ab initio* calculations on the coupled cluster level showed that the barriers from allyl to allene and to 2-propenyl are comparable and that a competition between the two channels can be expected. From the time-delay scans, rate constants of $>1 \times 10^8$ s⁻¹ for allene formation and 4×10^7 s⁻¹ for isomerization to 2-propenyl were determined, corresponding to a branching ratio of 2.5:1. RRKM calculations yielded a similar ratio of 2.3:1 for the two rate constants. Thus we conclude that the relative branching ratio for the two processes lies between 2:1 and 3:1 in favor of direct allene formation from allyl. From the experimental rates an activation barrier of 66 ± 1 kcal/mol for the 1,2 hydrogen shift to 2-propenyl is deduced, in agreement with the *ab initio* value.

From the FWHM of the measured Doppler profiles, a translational energy release of 14 ± 1 kcal/mol is calculated. For allene this corresponds to 24% of the excess energy being released as translation, for propyne this corresponds to 23%. This is substantially larger than expected from a prior distribution or RRKM calculations, but can be explained by the relatively large reverse activation barrier of 7 kcal/mol for the allyl→allene reaction. The energy of the reverse barrier will be preferentially released as translation.

ACKNOWLEDGMENTS

We would like to thank Thomas Gilbert for his contributions to the early part of this work and for working out the synthesis of the tetradeuterioallyliodide. Financial support from the Schweizerische Nationalfonds and the ETH Zürich is gratefully acknowledged.

APPENDIX: SYNTHESIS OF THE DEUTERATED PRECURSORS

For the experiments investigating the site specificity of the hydrogen loss, two different isotopically labeled precursors were employed. 2-deuterioallyliodide was synthesized from propargyl alcohol and LiAlD_4 , following the procedure described before.¹⁰

1,1,3,3-tetradeuterioallyliodide was synthesized in the following way: Please note that the first three steps were repeated several times before the fourth reaction was carried out.

- (1) 1,1-dideuterioprop-2-yn-1-ol: A solution of 47.1 g ethyl propiolate in 300 ml of ether was added dropwise to 15 g LiAlD_4 in 600 ml diethylether at -78° over a period of 4 h. The mixture was stirred overnight. After adding 15 ml H_2O dropwise, the mixture was brought to room temperature. 15 ml of a 15% NaOH solution and then 45 ml of H_2O were added. The precipitate was filtered off and washed with ether. The combined ethereal fractions were evaporated and distilled, yielding 28 g of 1,1-dideuterioprop-2-yn-1-ol, **1**, at $91\text{--}101^\circ$ at 1 atm.
- (2) 1,1-dideuterio-1-trimethylsiloxy-prop-2-yn: In order to protect the alcohol functionality, 40.6 g TMS-chlorid was added to a mixture of 21.7 g of **1** and 37.8 g $\text{N}(\text{C}_2\text{H}_5)_3$ in 200 ml pentane, stirred for 2 h at 0° , then 20 min at room temperature. The precipitate was filtered off and washed with pentane. The pentane fraction was distilled at 1 atm, yielding 16.6 g (34%) of the TMS-ether, **2**, at 90° .
- (3) 1,1,3-trideuterioprop-2-yn-1-ol: In the next step, the TMS ether was deprotonated with 95.5 ml of a 2 M solution of *n*-butyl lithium in hexane, which was added dropwise to **2** in 150 ml of THF. The reaction was carried out under Ar atmosphere at -78° . Subsequently, the TMS-ether was cleaved by adding 18.8 ml of a 38% $\text{DCI}/\text{D}_2\text{O}$ solution, yielding the 1,1,3-trideuterioprop-2-yn-1-ol, **3**. It was extracted by adding 200 ml of both CH_2Cl_2 and H_2O , separating the aqueous phase and washing it with CH_2Cl_2 . Upon distillation at $92\text{--}98^\circ$ and 1 ATM, 5.4 g of **3** were obtained.
- (4) 1,1,3,3-tetradeuterioprop-2-enol: In the next step, 11.4 g of **3** in 100 ml of ether were added dropwise to 8.9 g LiAlH_4 in 400 ml of ether under Ar atmosphere at 0° . The mixture was subsequently refluxed for 18 h. Then 45.6 g D_2O were added at room temperature. The lithium salt formed in the reaction was filtered off and washed with ether. The combined ethereal fractions were evaporated in order to obtain 5.1 g of 1,1,3,3-tetradeuterioprop-2-enol, the tetradeuterated allyl alcohol.

- (5) 1,1,3,3-tetradeuterio-1-iodoprop-2-ene: The alcohol was converted to the iodide by a modification of the Landauer and Rydon procedure.⁵⁸ 5.1 g of the alcohol were stirred with 17.7 g CH_3I in 25.5 g triphenylphosphite for one day under Ar at 75° , generating the 1,1,3,3- D_4 allyliodide. This was distilled off at 120 Torr/ $32\text{--}34^\circ$ yielding around 4.2 g (17% yield) of the precursor for our experiments.

For all substances NMR spectra were recorded that are available as supplementary material.³⁷

- ¹K. M. Leung and R. P. Lindstedt, *Combust. Flame* **102**, 129 (1995).
- ²S. D. Thomas, A. Bhargava, P. R. Westmoreland, R. P. Lindstedt, and G. Skevis, *Bull. Soc. Chim. Belg.* **105**, 501 (1996).
- ³E. Hirota, C. Yamada, and M. Okunishi, *J. Chem. Phys.* **97**, 2963 (1992).
- ⁴D. Uy, S. Davis, and D. J. Nesbitt, *J. Chem. Phys.* **109**, 7793 (1998).
- ⁵C. L. Currie and D. A. Ramsay, *J. Chem. Phys.* **45**, 488 (1966).
- ⁶J. W. Hudgens and C. S. Dulcey, *J. Phys. Chem.* **89**, 1505 (1985).
- ⁷A. D. Sappay and J. C. Weisshaar, *J. Phys. Chem.* **91**, 3731 (1987).
- ⁸D. W. Minsek, J. A. Blush, and P. Chen, *J. Phys. Chem.* **96**, 2025 (1992).
- ⁹J. A. Blush, D. W. Minsek, and P. Chen, *J. Phys. Chem.* **96**, 10150 (1992).
- ¹⁰D. W. Minsek and P. Chen, *J. Phys. Chem.* **97**, 13375 (1993).
- ¹¹H.-J. Deyerl, T. Gilbert, I. Fischer, and P. Chen, *J. Chem. Phys.* **107**, 3329 (1997).
- ¹²P. Chen, in *Unimolecular and Bimolecular Reaction Dynamics*, edited by C. Y. Ng, T. Baer, and I. Powis (Wiley, New York, 1994).
- ¹³*CRC Handbook of Chemistry and Physics*, edited by D. A. Lide (CRC, Boca Raton, 1994).
- ¹⁴H. Clauberg, D. W. Minsek, and P. Chen, *J. Am. Chem. Soc.* **114**, 99 (1992).
- ¹⁵T. Schultz and I. Fischer, *J. Chem. Phys.* **109**, 5812 (1998).
- ¹⁶R. Schmiedl, H. Dugan, W. Meier, and K.-H. Welge, *Z. Phys. A* **304**, 137 (1982).
- ¹⁷U. Gerlach-Meyer, E. Linnebach, K. Kleinermanns, and J. Wolfrum, *Chem. Phys. Lett.* **133**, 113 (1987).
- ¹⁸K. Tsukiyama and R. Bersohn, *J. Chem. Phys.* **86**, 745 (1987).
- ¹⁹S. Satyapal, G. W. Johnston, R. Bersohn, and I. Oref, *J. Chem. Phys.* **93**, 6398 (1990).
- ²⁰B. Koplitz, Z. Xu, D. Baugh, S. Buelow, D. Häusler, J. Rice, H. Reisler, C. X. W. Quiang, M. Noble, and C. Wittig, *Faraday Discuss. Chem. Soc.* **82**, 125 (1986).
- ²¹See, for example, H.-R. Volpp and J. Wolfrum, in *Gas-Phase Chemical Reaction Systems*, Springer Series in Chemical Physics, Vol. 61, edited by J. Wolfrum, H.-R. Volpp, R. Rannacher, and J. Warnatz (Springer, Berlin, 1996), and references therein.
- ²²E. F. Cromwell, A. Stolow, M. J. J. Vrakking, and Y. T. Lee, *J. Chem. Phys.* **97**, 4029 (1992).
- ²³P. Chen, S. D. Colson, W. A. Chupka, and J. A. Berson, *J. Phys. Chem.* **90**, 2319 (1986).
- ²⁴D. W. Kohn, H. Clauberg, and P. Chen, *Rev. Sci. Instrum.* **63**, 4003 (1992).
- ²⁵H. Zacharias, H. Rottker, J. Danon, and K. H. Welge, *Opt. Commun.* **37**, 15 (1981).
- ²⁶T. Schultz and I. Fischer, *J. Chem. Phys.* **107**, 8197 (1997).
- ²⁷J. Park, R. Bersohn, and I. Oref, *J. Chem. Phys.* **93**, 5700 (1990).
- ²⁸R. D. Levine and R. B. Bernstein, *Molecular Reaction Dynamics and Chemical Reactivity* (Oxford University Press, New York, 1987).
- ²⁹Aa. S. Sudbó, P. A. Schulz, E. R. Grant, Y. R. Shen, and Y. T. Lee, *J. Chem. Phys.* **70**, 912 (1979).
- ³⁰W. L. Hase and D. L. Bunker, QCOMP 082.
- ³¹S. W. North, D. A. Blank, J. D. Gezelter, C. A. Longfellow, and Y. T. Lee, *J. Chem. Phys.* **102**, 4447 (1995).
- ³²D. H. Mordaunt, D. L. Osborn, and D. M. Neumark, *J. Chem. Phys.* **108**, 2448 (1998).
- ³³G. E. Busch and K. R. Wilson, *J. Chem. Phys.* **56**, 3626 (1972).
- ³⁴T. Baer and W. L. Hase, *Unimolecular Reaction Dynamics* (Oxford University Press, New York, 1996).
- ³⁵J. L. Brum, S. Deshmukh, Z. Wang, and B. Koplitz, *J. Chem. Phys.* **98**, 1178 (1993).

- ³⁶K. A. Holbrook, M. J. Pilling, and S. H. Robertson, *Unimolecular Reactions* (Wiley, Chichester, 1996).
- ³⁷See AIP Document No. PAPS JCPSA6-110-010903 for 17 pages of calculational details and NMR spectra. Order by PAPS number and journal reference from American Institute of Physics, Physics Auxillary Publication Service, 500 Sunnyside Boulevard, Woodbury, NY 11797-2999. Fax: 516-576-2223, e-mail: paps@aip.org. The price is \$1.50 for each microfiche (98 pages) or \$5.00 for photocopies of up to 30 pages, and \$0.15 for each additional page over 30 pages, Airmail additional. Make checks payable to the American Institute of Physics.
- ³⁸GAUSSIAN 94 (Revision C.3), M. J. Frisch, G. W. Trucks, H. B. Schlegel, P. M. W. Gill, B. G. Johnson, M. A. Robb, J. R. Cheeseman, T. Keith, G. A. Petersson, J. A. Montgomery, K. Raghavachari, M. A. Al-Laham, V. G. Zakrzewski, J. V. Ortiz, J. B. Foresman, J. Cioslowski, B. B. Stefanov, A. Nanayakkara, M. Challacombe, C. Y. Peng, P. Y. Ayala, W. Chen, M. W. Wong, J. L. Andres, E. S. Replogle, R. Gomperts, R. L. Martin, D. J. Fox, J. S. Binkley, D. J. Defrees, J. Baker, J. P. Stewart, M. Head-Gordon, C. Gonzalez, and J. A. Pople (Gaussian, Inc., Pittsburgh PA, 1995).
- ³⁹J. D. Getty, M. J. Burmeister, S. G. Westre, and P. B. Kelly, *J. Am. Chem. Soc.* **113**, 801 (1991).
- ⁴⁰G. Maier, H.-P. Reisenauer, B. Rohde, and K. Dehnicke, *Chem. Ber.* **116**, 732 (1983).
- ⁴¹T. H. Dunning, Jr., *J. Chem. Phys.* **90**, 1007 (1989).
- ⁴²S. Olivella, A. Solé, and J. M. Bofill, *J. Am. Chem. Soc.* **112**, 2160 (1990).
- ⁴³G. Greig and J. C. J. Thynne, *Trans. Faraday Soc.* **63**, 1369 (1967).
- ⁴⁴We like to thank Prof. M. Quack for making this program available to us.
- ⁴⁵H.-G. Korth, H. Trill, and R. Sustmann, *J. Am. Chem. Soc.* **103**, 4483 (1981).
- ⁴⁶K. Holtzhaer, C. Cometta-Morini, and J. F. M. Oth, *J. Phys. Org. Chem.* **3**, 219 (1990).
- ⁴⁷V. A. Radzig, L. Yu. Ustynyuk, N. Yu. Osokina, V. I. Pergushov, and M. Ya. Mel'nikov, *J. Phys. Chem. A* **102**, 5220 (1998).
- ⁴⁸G. Maier and S. Senger, *Angew. Chem. Int. Ed. Engl.* **33**, 558 (1994).
- ⁴⁹P. Merlet, S. D. Peyerimhoff, R. J. Buenker, and S. Shih, *J. Am. Chem. Soc.* **96**, 959 (1974).
- ⁵⁰M. Yamaguchi, *J. Mol. Struct.: THEOCHEM* **365**, 143 (1996).
- ⁵¹Z. Wang, M. G. Mathews, and B. Koplitz, *J. Phys. Chem.* **99**, 6913 (1995).
- ⁵²M. Karni, I. Oref, S. Barzilai-Gilboa, and A. Lifshitz, *J. Phys. Chem.* **92**, 6924 (1988).
- ⁵³R. E. Continetti, D. R. Cyr, D. L. Osborn, D. J. Leahy, and D. M. Neumark, *J. Chem. Phys.* **99**, 2616 (1993).
- ⁵⁴D. L. Osborn, D. J. Leahy, E. M. Ross, and D. M. Neumark, *Chem. Phys. Lett.* **235**, 484 (1995).
- ⁵⁵D. L. Osborn, H. Choi, D. H. Mordaunt, R. T. Bise, D. M. Neumark, and C. McMichael Rohlfling, *J. Chem. Phys.* **106**, 3049 (1997).
- ⁵⁶K. A. Hanold, C. R. Sherwood, M. C. Garner, and R. E. Continetti, *Rev. Sci. Instrum.* **66**, 5507 (1995).
- ⁵⁷K. A. Hanold, M. C. Garner, and R. E. Continetti, *Phys. Rev. Lett.* **77**, 3335 (1996).
- ⁵⁸S. R. Landauer and H. N. Rydon, *J. Chem. Soc.* **1953** (2224).